UCRL-16922

University of California

Ernest O. Lawrence Radiation Laboratory

STRENGTHENING MECHANISMS OF ULTRA-HIGH-STRENGTH AUSTENITIC STEEL

TWO-WEEK LOAN COPY

This is a Library Circulating Copy which may be borrowed for two weeks. For a personal retention copy, call Tech. Info. Division, Ext. 5545

DISCLAIMER

This document was prepared as an account of work sponsored by the United States Government. While this document is believed to contain correct information, neither the United States Government nor any agency thereof, nor the Regents of the University of California, nor any of their employees, makes any warranty, express or implied, or assumes any legal responsibility for the accuracy, completeness, or usefulness of any information, apparatus, product, or process disclosed, or represents that its use would not infringe privately owned rights. Reference herein to any specific commercial product, process, or service by its trade name, trademark, manufacturer, or otherwise, does not necessarily constitute or imply its endorsement, recommendation, or favoring by the United States Government or any agency thereof, or the Regents of the University of California. The views and opinions of authors expressed herein do not necessarily state or reflect those of the United States Government or any agency thereof or the Regents of the University of California.

Special thesis

UCRL-16922

UNIVERSITY OF CALIFORNIA

Lawrence Radiation Laboratory
Berkeley, California

AEC Contract No. W-7405-eng-48

STRENGTHENING MECHANISMS OF ULTRA-HIGH-STRENGTH AUSTENITIC STEEL

Dieter Fahr

(M. S. Thesis)

June 1966

TABLE OF CONTENTS

ABSTRACT

I. INTRODUCTION 1

II. EXPERIMENTAL PROCEDURE 3

III. RESULTS AND DISCUSSION 5

A. Amount of Deformation 6

B. Deformation Temperature 10

C. The Thermal and Mechanical Stabilization of Austenite ... 11

IV. SUMMARY AND CONCLUSIONS 13

V. ACKNOWLEDGEMENTS 15

VI. REFERENCES 16

VII. FIGURE CAPTIONS 18

APPENDIX 20

STRENGTHENING MECHANISMS OF ULTRA-HIGH-STRENGTH AUSTENITIC STEEL

Dieter Fahr

Inorganic Materials Research Division, Lawrence Radiation Laboratory,
Department of Mineral Technology, College of Engineering
University of California, Berkeley, California

June 1966

ABSTRACT

This investigation was concerned with the development of a high strength stable austenitic steel. A composition which was expected to show stabilization and dispersion strengthening as results of thermomechanical processing was selected. The principle variables investigated were the amount and temperature of deformation and the temperature of aging after deformation.

The mechanical properties were most sensitive to the amount of deformation. Both strength and ductility increased with prior deformation. Within the ranges studied, the deformation and aging temperatures had a smaller effect on the properties.

The stabilization of the austenite also depended on the amount of reduction. With large deformations, the M_s temperature was lowered from -50°C (undeformed) to about -196°C.

Optimum thermomechanical processing produced a stable austenitic steel with the following mechanical properties, 180,000 psi yield strength, 270,000 psi ultimate tensile strength, 20% elongation and 40% reduction in area.

I. INTRODUCTION

Iron based alloys are either body-centered-cubic or face-centered-cubic in structure each being characterized by a particular set of mechanical properties. Body-centered-cubic (bcc) alloys have, in general, high strength and relatively low ductility, while the face-centered-cubic (fcc) or austenitic alloys have low strength but high ductility. Furthermore, fcc alloys are not subject to a ductile-to-brittle fracture transition and, in general, have higher corrosion resistance. These properties account for the selection of austenitic steel in many applications. The utility of these steels would be greatly enhanced if their strength could be significantly increased.

Attempts to increase the strength of austenitic steels have resulted largely in loss of ductility and corrosion resistance. For example, these steels can be strengthened by cold working. When the steel is stable against strain induced transformation to martensite, the strengthening by cold work is small. When this transformation occurs the strengthening is large but the ductility is lost. In another class of austenitic steels, the strengthening is obtained by controlled transformation to a polyphase structure, i.e., with suitable compositions and heat treatments a mixed microstructure of austenite and martensite results. Although the requisite control of composition is difficult to maintain, the balance of strength and ductility is good, e.g., yield strengths of 200,000 psi and elongations of 20%.[1] In general, these polyphase alloys have less corrosion resistance than the single phase alloys.

Another approach to strengthening has been to induce precipitation on structural defects in the austenitic matrix. Honeycombe et al.[2] have shown that by suitable selection of matrix composition and precipitating

carbide it was possible to form a high volume fraction of intersecting sheets of fine precipitate. A sixfold increase in yield strength was obtained in high purity alloys. This technique is promising since it does not depend on partial transformation of the matrix to martensite with the associated loss of corrosion resistance. To prevent athermal decomposition, Honeycombe et al. used very highly alloyed steels.[2]

In the present study a lower alloy austenite was stabilized against transformation by a thermomechanical treatment which simultaneously produced the strengthening precipitate. It has been suggested[3] that precipitates produced during thermomechanical treatment may be more effective strengthening agents than those produced by heat treatment alone. In this way it was hoped to obtain a dispersion hardened low alloy stable austenite, thus retaining favorable corrosion resistance and fracture characteristics.

II. EXPERIMENTAL PROCEDURE

The alloy used in this study was designed on the basis of previous work with high strength austenitic/martensitic steels. An austenite with a high work hardening rate, high stability, and extensive precipitation hardening with deformation was desired. The steel was prepared by induction melting high purity elements in a helium atmosphere. The composition is shown in Table I. The ingots were hot forged to 1 × 3/8", and annealed. The material was then rolled to thicknesses which would produce 0.050" thick specimens after further reductions of 20, 40, 60 and 80%. This material was austenitized in argon at 1100°C for 30 min. and slowly cooled. The samples were austenitic at room temperature.

Deformation temperatures of 450, 500, and 550°C were selected on the basis of previous work with similar alloys. Deformation was effected by rolling (heated rolls) and reheating the specimens in an electric furnace between passes.* About 45 minutes were required to complete the 80% reduction in thickness. After deformation the specimens were immediately water quenched. Some specimens were tested in this condition; the remainder were refrigerated in liquid nitrogen and subsequently aged at temperatures between 450 and 600°C. Undeformed specimens were subjected to similar heat treatments.

Tensile specimens were prepared and tested at room temperature on an Instron testing machine using a cross head speed which gave an initial strain rate of 0.075/min.

To determine if the preliminary rolling influenced the results, additional specimens were prepared. One group was machined from as forged condition to the starting thickness; a second group was rolled in a direction

---

* In this way the actual deformation temperature was controlled within about ± 10°C.

perpendicular to the final rolling direction. No significant difference in properties were observed with these treatments.

The microstructure was examined by optical and electron microscopy. Carbide extraction replicas were prepared by the single stage technique.[4] The carbon film was removed by electrolytic etching with a 10% oxalic acid solution.

II. EXPERIMENTAL PROCEDURE

The alloy used in this study was designed on the basis of previous work with high strength austenitic/martensitic steels. An austenite with a high work hardening rate, high stability, and extensive precipitation hardening with deformation was desired. The steel was prepared by induction melting high purity elements in a helium atmosphere. The composition is shown in Table I. The ingots were hot forged to 1 × 3/8", and annealed. The material was then rolled to thicknesses which would produce 0.050" thick specimens after further reductions of 20, 40, 60 and 80%. This material was austenitized in argon at 1100°C for 30 min. and slowly cooled. The samples were austenitic at room temperature.

Deformation temperatures of 450, 500, and 550°C were selected on the basis of previous work with similar alloys. Deformation was effected by rolling (heated rolls) and reheating the specimens in an electric furnace between passes.* About 45 minutes were required to complete the 80% reduction in thickness. After deformation the specimens were immediately water quenched. Some specimens were tested in this condition; the remainder were refrigerated in liquid nitrogen and subsequently aged at temperatures between 450 and 600°C. Undeformed specimens were subjected to similar heat treatments.

Tensile specimens were prepared and tested at room temperature on an Instron testing machine using a cross head speed which gave an initial strain rate of 0.075/min.

To determine if the preliminary rolling influenced the results, additional specimens were prepared. One group was machined from as forged condition to the starting thickness; a second group was rolled in a direction

---

* In this way the actual deformation temperature was controlled within about ± 10°C.

perpendicular to the final rolling direction. No significant difference in properties were observed with these treatments.

The microstructure was examined by optical and electron microscopy. Carbide extraction replicas were prepared by the single stage technique.[4] The carbon film was removed by electrolytic etching with a 10% oxalic acid solution.

III. RESULTS AND DISCUSSION

The mechanical properties of this austenitic steel are clearly the result of processes occurring during the thermomechanical treatments. In the absence of detailed structural studies of alloys whose composition and processing are controlled over a wide range, it is not possible to evaluate quantitatively the contributions of the various strengthening mechanisms. However, factors that are significant in this study may be considered by examining first the influence of room and elevated temperature deformation on the properties of single phase austenite; secondly, the influence of precipitation of second phase particles in the deformed austenite, and finally, the effect of deformation and precipitation on the stability of the austenite.

The strength and structure of cold worked austenite has been studied by numerous investigators.[5,6,7] In the absence of a thermal or isothermal phase transformation, the increase in yield strength of austenite is directly proportional to the amount of cold work. In an alloy with low carbon or nitrogen content this strengthening can be as large as the produced by transformation of the alloy to martensite.[8] As the temperature of deformation is increased, the dislocations become mobile enough to form small angle boundaries. The spacing of these boundaries is directly related to the deformation temperature. Since the strengthening effect of the boundaries is predicted to be inversely proportional to their spacing,[9] the strength of deformed single phase austenite is expected to decrease with increasing deformation temperature.

Higher strengths than those attainable by deformation alone can be obtained by combining deformation with precipitation. This possibility may be considered in steels which contain carbon, with or without alloy

carbide formers. The properties of these alloys were studied as a function of deformation temperature. As Thomas et al.[11] have shown, the strengthening of both carbide and non-carbide forming alloys is identical when the deformation is introduced at room temperature. At higher temperatures, the steels containing alloy carbide formers strain hardened more rapidly and subsequently exhibited a higher yield strength at room temperature. These alloys showed evidence of precipitation of alloy carbides and a higher density of dislocations than the steel without alloy carbide formers. Thomas et al. postulate that the carbides serve both to pin existing dislocations and to increase the rate of dislocation multiplication. The strength at room temperature is viewed as a sum ot two contributions: dispersion hardening and a high dislocation density.

The factors of importance in the present investigation are similar to those discussed above. The steel studied contained sufficient alloy carbide forming elements to combine with the carbon present; it was deformed in a similar temperature range, and remained austenitic to room temperature. The mechanical properties and structure are therefore considered in terms of the same strengthening mechanisms. The three processing variables employed were the amount and temperature of deformation, and the subsequent aging temperature.

A. Amount of Deformation

The mechanical properties were most influenced by the amount of deformation, as shown in Figs. 1, 2, and 3 for a deformation temperature of 450°C.* The yield strength, Fig. 1, increased approximately linearly with the amount of reduction in thickness. The ultimate strength increased rapidly up to 40% reduction of thickness and more slowly thereafter.

---

* All mechanical property data are tabulated in the Appendix.

Similar behavior was observed at the other deformation temperatures employed. This dependence of strength on amount of prior deformation would be expected if the dislocation density were the sole contributing factor. However, precipitation occurs during deformation and also contributes to the strength. The relative importance of these two factors cannot be assessed on the basis of the present experiments.

An additional factor is the stability of the austenite as influenced by the amount of deformation. Qualitative magnetic measurements indicated that the amount of martensite formed on refrigeration to liquid nitrogen temperature decreased with increasing deformation. If it can be assumed that the strengthening effect of this second phase is proportional to the amount present, then its contribution would be less at higher deformations. This is confirmed by the lack of response to refrigeration of the specimens deformed 80%.

The structures produced by different amounts of deformation at 450°C are shown in Figs. 4 and 5. The density of decorated slip lines is clearly greater at the higher deformation. If sufficient precipitation occurs to pin the network of dislocations associated with the slip lines, the structure with the smaller slip line spacing, i.e., greater deformation, would be expected to have the higher strength, as is observed.

The precipitate shown in Figs. 4 and 5 was studied by selected area electron diffraction from the extraction replicas. The patterns obtained (see Fig. 6) were best indexed as those of MoC and Cr_7C_3. The carbides could have formed either during deformation or the subsequent aging treatment. The fact that no strengthening was observed upon aging the deformed specimens strongly suggests that the carbides formed during deformation.

This is consistent with the well known effect of deformation on the kinetics of precipitation reactions.[12]

It is of interest that the ductility (Figs. 2 and 3) tends to increase with increasing prior deformation. In dispersion hardened systems, where strength is controlled by the particle spacing, and the dislocation density is relatively constant, the ductility decreases with increasing strength. However, in structures produced by thermo-mechanical processing (e.g., ausform steels, dynamically strain aged steels, and the present alloy) the inverse relationship between strength and ductility is not observed. This suggests that a high dislocation density is desirable for the best combination of strength and ductility. The large increase in ductility in the present study may be due partly to martensite formed during the room temperature test and partly to elimination of embrittling grain boundary precipitates, which are observed in the undeformed alloy. (see Fig. 7).*

Martensite formation causes a further increase in dislocation density and thus leads to increased strain hardening. If martensite is harder than the parent austenite the rate of strain hardening is increased even more. High strain hardening prevents early necking and thus favors greater ductility. If the martensite has a greater specific volume than the parent austenite, as is the case in alloys containing interstitial solutes, a sudden extension of the specimen accompanies the transformation. In a "hard" testing machine, this extension appears as a load drop, i.e., a serrated stress strain curve results. Such behavior was observed in some specimens in the present study, as is discussed in a later section. Qualitative magnetic measurements indicated that some transformation to marten-

* The undeformed alloys were characterized by both low yield strength (less than 100,000 psi) and negligible ductility.

site occurred during testing of these specimens, although the amount of martensite formed is not known.

The effect of prior deformation on the ductility is seen to be due to the dislocations introduced which provide alternate nucleation sites for carbide precipitation, and thus reduce the supersaturation at the grain boundaries.

B. Deformation Temperature

Preliminary experiments revealed that the strengthening effect of deformation was most pronounced in the temperature range of 450-550°C. At much lower temperatures, e.g., ambient, the diffusivity is inadequate for precipitation to occur, thus the strengthening is limited to normal work hardening of a single phase material. At temperatures above the optimum range, recovery, coarsening of the precipitate, and eventually recrystallization, occur with consequent loss os strength. Within the selected range of temperatures of 450-550°C, the properties were relatively insensitive to deformation temperature, as seen in Figs. 8-10. Similar behavior has been observed in studies of the effect of processing on ausform steel.[13] The only microstructural difference observed was an apparent coarsening of the precipitate with increasing deformation temperature as seen in Fig. 11.

A tentative explanation of this behavior is suggested by the changes occurring in the microstructure with deformation temperature. The morphology of the precipitate as influenced by temperature will be considered first in the highly deformed alloy. The precipitate is in the form of long thin plates at low deformation temperatures, as shown in Fig. 15a. Brittle particles with this morphology tend to act as effective sites for the nucleation and growth of cracks. With increasing deformation temperature, or equivalently, increasing aging temperature, the plates break up into strings of smaller more rounded particles as shown in Fig. 15b. This change would not have a large effect on strength but would be expected to increase the ductility significantly. In specimens deformed smaller amounts, however, the ductility is controlled by the grain boundary precipitate. Higher deformation temperatures or aging temperatures promote the growth of this precipitate and thus induce further embrittlement.

C. The Thermal and Mechanical Stabilization of Austenite

As austenite is cooled, its stability relative to martensite of the same composition decreases. At the transformation temperature (M_s) which depends on composition, the austenite is sufficiently less stable than martensite, so that the activation barrier is overcome and martensite is formed. Thus, changes in the M_s temperature of an alloy reflect either changes in the matrix composition, e.g., by precipitation, or changes in the height of the activation barrier.[14,15] Since most alloying elements lower the M_s, precipitation tends to decrease the stability of austenite. This effect may be overbalanced if the precipitate pins the interface between martensite embryos and the matrix, thus reducing the martensite nucleation rate. Deformation stabilizes the austenite through the formation of a cell structure, which provides barriers to the growth of martensite plates. This stabilization increases if the cell structure is locked by precipitate.

The present alloy has an M_s of about -50°C after austenitizing at 1000°C and water quenching to room temperature. The M_s decreased with increasing amounts of deformation. After 80% deformation, the M_s was in the vicinity of liquid nitrogen temperature (-196°C). This change is two to three times greater than generally observed in stabilization experiments.[16] This large stabilization can be understood in terms of the precipitate structure seen in the extraction replicas (Figs. 4 and 5). The matrix is divided into small volumes by the carbide rods or plates, which formed on the slip structure. Thus the size of the martensite plate which can form from a particular embryo, and thus the total amount of martensite formed, is limited.

The highly deformed specimens exhibited a serrated stress-strain curve on final testing at room temperature. This was attributed to the formation of stress induced martensite. A deformation of 1-2% by rolling at room temperature prior to the test reduced the extent of the serrations. A similar deformation at liquid nitrogen temperature completely eliminated the effect. Apparently that portion of the austenite which was unstable in the presence of stress was transformed by these treatments. It is not clear why specimens, deformed a smaller amount, did not exhibit the serrated stress-strain behavior.

IV. SUMMARY AND CONCLUSIONS

The objective of this study was to produce a high strength stable austenitic steel. Previous experimental work in this laboratory and elsewhere suggested that thermomechanical processing might produce the strengthening and stabilization required. The composition of the steel was designed to include both sufficient alloying elements to depress the M_s below room temperature and carbide forming elements for dispersion hardening. Three principal variables were investigated; the amount and temperature of deformation, and the temperature of aging after deformation.

The variable found to be most important was the amount of deformation. Both the strength and the ductility increased with increased deformation. This behavior was interpreted in terms of both dislocation density and the amount of precipitation. The yield strength and ductility were approximately doubled at the highest degree of deformation.

The strength and elongation were insensitive to the temperatures of deformation and aging. The reduction in area, however, has highly sensitive to these process variables. This behavior was rationalized on the basis of carbide morphology.

The precipitates formed during processing were identified as MoC and Cr_7C_3 by selected area electron diffraction. Appreciable austenite stabilization was obtained by simultaneous deformation and precipitation. The degree of stabilization increased with increasing deformation. By optimum processing the M_s temperature was depressed from -50°C to about -196°C, although the M_d remained above room temperature. The stabilization was attributed to the subdivision of the austenite grains into micron-sized units by decorated slip bands.

Serrated stress-strain curves were obtained during room temperature testing after certain processing conditions. This phenomena was ascribed to the formation of stress-induced martensite. These serrations were diminished in magnitude by small amounts of rolling at room or lower temperatures prior to testing.

It has been demonstrated that high strength (about 200,000 psi) with unusually high ductility (25% elongation) can be obtained in stable austenitic steels. By way of comparison, a martensitic steel of the same strength would have less than half the ductility.

Future work encompasses studies that hopefully will lead to a greater understanding of austenite stabilization. These will include the effects of composition and structure in both simple and complex alloys. Attempts will be made to assess the relative contributions of thermal and mechanical stabilization.

V. ACKNOWLEDGEMENTS

The author is deeply grateful to Dr. V. F. Zackay and Dr. R. A. Busch for their research guidance, encouragements and support throughout the course of this investigation.

This work was performed under the auspices of the United States Atomic Energy Commission through the Inorganic Materials Research Division of the Lawrence Radiation Laboratory, Berkeley, California.

VI. REFERENCES

1. T. H. McCunn, G. N. Aggen and R. A. Lula, Structure and Properties of Ultrahigh Strength Steels, ASTM Spec. Tech. Pub. No. 370, 1965, p. 78.
2. R. W. K. Honeycombe, H. J. Harding, and J. J. Irani, High Strength Materials, V. F. Zackay, ed., (John Wiley and Sons, Inc., New York, 1965) p. 213.
3. A. McEvily, R. Bush, F. Schaller, and D. Schmatz, Trans. ASM, 56, 753 (1963).
4. D. Kay, Techniques for Electron Microscopy, (Blackwell Scientific Publishers, Oxford, 1961) p. 99.
5. J. Christian, J. Gruner, and L. Girton, Trans. ASM, 57, 199 (1964).
6. S. Floreen and G. Tuffnell, Trans. ASM, 57, 310 (1964).
7. G. Powell, E. Marshall and W. Backofen, Trans. ASM, 50, 478 (1958).
8. D. Schmatz, F. W. Schaller, and V. F. Zackay, The Relation Between the Structure and Mechanical Properties of Metals, (HMSO, London, 1963), Vol. II.
9. J. Friedel, Internal Stresses and Fatigue in Metals, G. M. Rassweiler and W. Grube, Eds., (Elsevier Publishing Co., Amsterdam, 1959) p. 234.
10. J. C. Li, Electron Microscopy and Strength of Crystals, G. Thomas and J. Washburn, Eds., (Interscience, New York, 1963) p. 713.
11. G. Thomas, D. Schmatz and W. Gerberich, High Strength Materials, V. F. Zackay, Ed., (John Wiley and Sons, Inc., New York, 1965) p. 251.
12. A. S. Keh and W. Leslie, Structure and Properties of Engineering Materials, H. H. Stadelmaier, Ed., (Interscience Publishers, New York, 1964) p. 208.

13. W. Gerberich, C. Martin and L. Raymond, Trans. ASM, 57, 324 (1964).

14. Physical Properties of Martensite and Bainite, I.S.I., Special Report No. 93, London, 1965.

15. G. Kraus and M. Cohen, Trans. AIME, 227, 278 (1963).

16. K. Kensman, Ph. D. Thesis, Stanford University, 1966.

VII. FIGURE CAPTIONS

Fig. 1 Yield and ultimate tensile strength at room temperature vs amount of reduction by rolling at 450°C. The temperatures of aging after reduction are indicated.

Fig. 2 Elongation at room temperature vs amount of reduction by rolling at 450°C. The temperatures of aging after reduction are indicated.

Fig. 3 Reduction in area at room temperature vs amount of reduction by rolling at 450°C. The temperatures of aging after reduction are indicated.

Fig. 4 Carbide extraction micrograph of specimen reduced 60% in thickness at 450°C, and aged at 450°C. Magnification 4000 ×.

Fig. 5 Carbide extraction micrograph of specimen reduced 80% in thickness at 450°C, and aged at 600°C. Magnification 4000 ×.

Fig. 6 Electron diffraction pattern obtained from carbide extraction replicas of deformed specimens. The pattern is best indexed as arising from MoC and Cr_7C_3.

Fig. 7 Optical micrograph of undeformed specimen aged at 450°C, showing the grain boundary precipitate which is believed to cause the brittleness of these specimens. Magnification 600 ×.

Fig. 8 Yield and ultimate tensile strength at room temperature vs the temperature of deformation. The temperature of aging after the reduction was 450°C. The amount of deformation is indicated.

Fig. 9 Elongation at room temperature vs the temperature of deformation. The temperature of aging after the reduction was 450°C. The amount of deformation is indicated.

Fig. 10 Reduction in area at room temperature vs the temperature of de-

formation. The temperature of aging after the reduction was 450°C. The amount of deformation is indicated.

Fig. 11 Optical micrographs of specimens deformed 80% by rolling. a)deformation temperature 450°C, b) deformation temperature 550°C. Magnification 600 ×.

Fig. 12 Yield and ultimate tensile strength at room temperature vs the temperature of aging after deformation at 450°C. The amounts of deformation are indicated.

Fig. 13 Elongation at room temperature vs the temperature of aging after deformation at 450°C. The amounts of deformation are indicated.

Fig. 14 Reduction in area at room temperature vs the temperature of aging after deformation at 450°C. The amounts of deformation are indicated.

Fig. 15 Optical micrographs of specimens deformed 80% at 450°C. a) aged at 450°C, b) aged at 500°C. Magnification 600×.

Fig. 16 Carbide extraction micrographs of specimens deformed 80% at 450°C. a) aged at 450°C, b) aged at 500°C. Magnification 4000×.

APPENDIX

Table I. Composition of steel

Element	Weight-%
Chromium	8.67
Nickel	8.08
Silicon	1.87
Manganese	0.81
Molybdenum	3.96
Carbon	0.28
Iron	balance

Table II. Deformation Temperature: 450°C

Tempering Temperature	Properties	Degree of Deformation 80%	60%	40%	20%
450°C	yield strength	181,000 psi	139,200 psi	125,000 psi	117,000 psi
	ultimate tensile strength	266,000 psi	230,000 psi	226,000 psi	155,000 psi
	hardness (R_c)	52	48.5	41.5	35.5
	elongation	23%	20%	29%	9%
	reduction in area	21%	22%	43.5%	29%
500°C	yield strength	177,200 psi	141,800 psi	119,000 psi	104,000 psi
	ultimate tensile strength	268,800 psi	250,000 psi	226,000 psi	145,200 psi
	hardness (R_c)	52	45.5	41.5	34.5
	elongation	21%	27%	24%	10%
	reduction in area	40%	49%	46.5%	20%
550°C	yield strength	171,200 psi	119,600 psi	115,600 psi	96,000 psi
	ultimate tensile strength	274,000 psi	248,000 psi	229,000 psi	115,000 psi
	hardness (R_c)	51	44	40.5	32
	elongation	23%	22%	24%	5%
	reduction in area	48.5%	40%	30%	11%
600°C	yield strength	143,200 psi	109,000 psi	96,200 psi	83,000 psi
	ultimate tensile strength	264,000 psi	249,000 psi	211,800 psi	144,300 psi
	hardness (R_c)	50	44	39.5	34.5
	elongation	18%	20%	16%	7%
	reduction in area	43%	30.5%	15%	16%

Table II. (continued) Deformation Temperature: 500°C

Tempering Temperatures	Properties	Degree of Deformation 80%	40%
450°C	yield strength	178,000 psi	131,000 psi
	ultimate tensile strength	271,000 psi	220,000 psi
	hardness (R_c)	51	41.5
	elongation	22%	27%
	reduction in area	33%	23%
500°C	yield strength	172,500 psi	127,300 psi
	ultimate tensile strength	271,000 psi	224,000 psi
	hardness (R_c)	51	40.5
	elongation	24%	28%
	reduction in area	40%	30%
550°C	yield strength	169,000 psi	115,000 psi
	ultimate tensile strength	276,000 psi	229,000 psi
	hardness (R_c)	50.5	40.5
	elongation	22%	24%
	reduction in area	46%	35%
600°C	yield strength	149,500 psi	103,500 psi
	ultimate tensile strength	267,800 psi	221,000 psi
	hardness (R_c)	50	40
	elongation	23%	18%
	reduction in area	38%	24%

Table II. (continued) Deformation Temperature: 550°C

Tempering Temperatures	Properties	Degree of Deformation 80%	40%
450°C	yield strength	166,800 psi	129,000 psi
	ultimate tensile strength	276,800 psi	215,000 psi
	hardness (R_c)	51	41.5
	elongation	22%	21%
	reduction in area	50.5%	23%
500°C	yield strength	165,200 psi	119,000 psi
	ultimate tensile strength	278,300 psi	229,000 psi
	hardness (R_c)	51	42
	elongation	24%	23%
	reduction in area	49%	30%
550°C	yield strength	158,000 psi	115,000 psi
	ultimate tensile strength	279,300 psi	191,500 psi
	hardness (R_c)	51	41.5
	elongation	23%	11%
	reduction in area	44%	19%
600°C	yield strength	150,000 psi	101,300 psi
	ultimate tensile strength	269,500 psi	221,800 psi
	hardness (R_c)	50	40.5
	elongation	18%	17%
	reduction in area	37%	18%

Table III.

Deformation Temperature: 450°C
Degree of Deformation: 80%
Quenched in LN
Tempered at 450°C for 30 Minutes

Mechanical Treatment before final deformation	Properties			
	yield strength	ultimate tensile strength	hardness (R_c)	elongation
rolled in direction of tensile axis	181,000 psi	266,000 psi	52	23%
rolled perpendicular to tensile axis	167,500 psi	258,000 psi	51	20%
milled to starting dimension	176,000 psi	271,500 psi	52	21%

Table IV. Undeformed Specimens

Thermal Treatment After Austenitizing at 1100°C	Properties			
	yield strength	ultimate tensile strength	hardness (R_c)	elongation
Slowly cooled in argon	41,000 psi	129,000 psi	3	23%
Quenched in H_2O (RT)	46,000 psi	115,800 psi	4.5	21%
Quenched in LN	106,000 psi	230,200 psi	39	23%
Quenched in LN - and tempered at 450°C	93,900 psi	166,000 psi	39	3%
Quenched in LN - and tempered at 500°C	95,300 psi	121,000 psi	40.5	2%
Quenched in LN - and tempered at 550°C	—	148,000 psi	38.5	1%
Quenched in LN - and tempered at 600°C	111,800 psi	219,000 psi	42	2%

Table V.

Deformation Temperature: 450°C
Degree of Deformation: 80%
Quenched in LN

Further Thermal Treatment	Properties			
	yield strength	ultimate tensile strength	hardness (R_c)	elongation
tempered at 450°C	181,000 psi	266,000 psi	52	23%
tempered at 400°C	173,500 psi	262,000 psi	51.5	18.5%
original deformation ⊥ to tensile axis				
tempered at 450°C	167,500 psi	258,000 psi	51	20%
tempered at 400°C	175,300 psi	267,000 psi	51	22%
milled down to starting dimension				
tempered at 450°C	176,000 psi	271,500 psi	52	21%
tempered at 400°C	172,000 psi	268,000 psi	51.5	20%
The following specimens were 79% deformed at 450°C and then quenched in LN				
1 more % deformed at LN-temp. no tempering	166,800 psi	270,000 psi	50.5	21%
tempered at 450°C (-30 min/and quenched again in LN to be deformed 1 more percent at LN-temperature)	180,500 psi	276,000 psi	53.5	20%

Table VI. Deformation Temperature: 450°C

Heat Treatment after Deformation	Properties	Degree of Deformation 80%	60%	40%
Quenched in H_2O(RT) No Tempering	yield strength	198,000 psi	132,200 psi	118,700 psi
	ultimate tensile strength	274,000 psi	237,800 psi	218,000 psi
	hardness (R_c)	50	45	40.5
	elongation	19%	27%	30%
Quenched in LN No Tempering	yield strength	190,700 psi	136,500 psi	123,800 psi
	ultimate tensile strength	271,000 psi	238,000 psi	219,500 psi
	hardness (R_c)	50	45	40
	elongation	22%	26%	33%
Deformation Temperature: 500°C				
Quenched in H_2O(RT) No Tempering	yield strength	174,600 psi		117,000 psi
	ultimate tensile strength	267,000 psi		189,000 psi
	hardness (R_c)	50.0		40.5
	elongation	22%		20%
Quenched in LN No Tempering	yield strength	173,800 psi		122,000 psi
	ultimate tensile strength	262,000 psi		209,000 psi
	hardness (R_c)	49.5		41
	elongation	24.5%		22%
Quenched in LN Tempered at 450°C	yield strength	178,000 psi		131,000 psi
	ultimate tensile strength	271,000 psi		220,000 psi
	hardness (R_c)	51		41.5
	elongation	22%		27%

Table VI. (continued) Deformation Temperature: 550°C

Heat Treatment After Deformation	Properties	Degree of Deformation 80%	40%
Quenched in H_2O(RT) No Tempering	yield strength	149,000 psi	132,500 psi
	ultimate tensile strength	269,500 psi	221,000 psi
	hardness (R_c)	49.5	41.5
	elongation	23%	29%
Quenched in LN No Tempering	yield strength	153,600 psi	130,500 psi
	ultimate tensile strength	277,500 psi	222,000 psi
	hardness (R_c)	49.5	41.5
	elongation	22%	27%
Quenched in LN Tempered at 450° C	yield strength	166,800 psi	129,000 psi
	ultimate tensile strength	276,800 psi	215,000 psi
	hardness (R_c)	51	41.5
	elongation	22%	21%

Table VII.

Earlier Experiments with Alloy No.6558 (Difference: 0.25% C compared to 0.28% C)

Deformation Temperature: 500°C
Degree of Deformation: ~83%

Heat Treatment After Deformation	Properties			
	yield strength	ultimate tensile strength	hardness (R_c)	elongation
Air cooled - no tempering	207,900 psi	282,300 psi	50	27%
Air cooled - quenched in LN no tempering	204,000 psi	281,000 psi	50	30%
Air cooled and quenched in LN tempered at 450°C	215,400 psi	291,000 psi	51	27%
Deformation Temperature: 600°C, Degree of Deformation: ~83%				
Air cooled - no tempering	179,300 psi	288,200 psi	49	25%
Air cooled and quenched in LN no tempering	186,000 psi	290,000 psi	50	25%
Air cooled and quenched in LN tempered at 450°C (30 min.)	185,400 psi	296,000 psi	50.5	26%

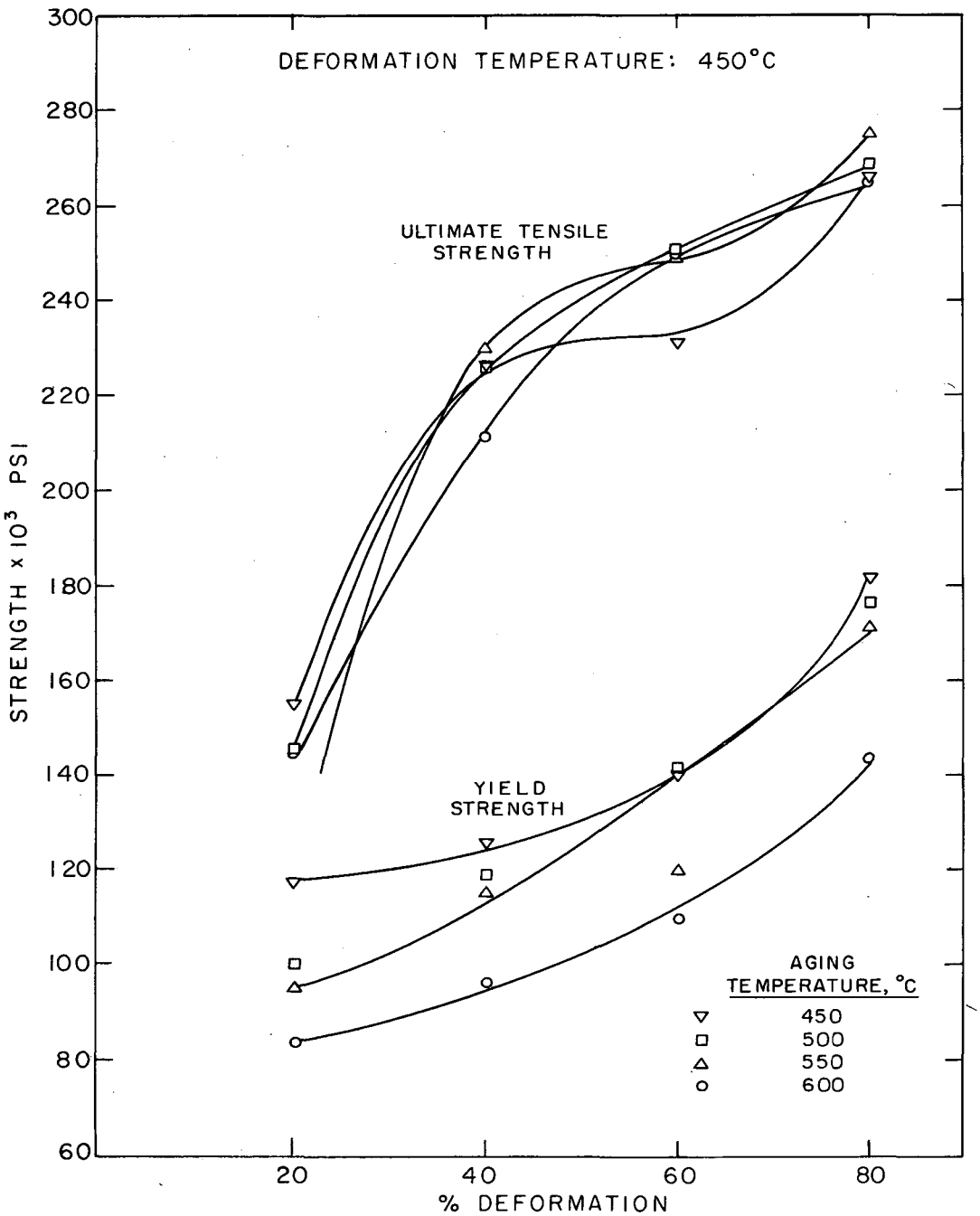

MUB-11005

Fig. 1

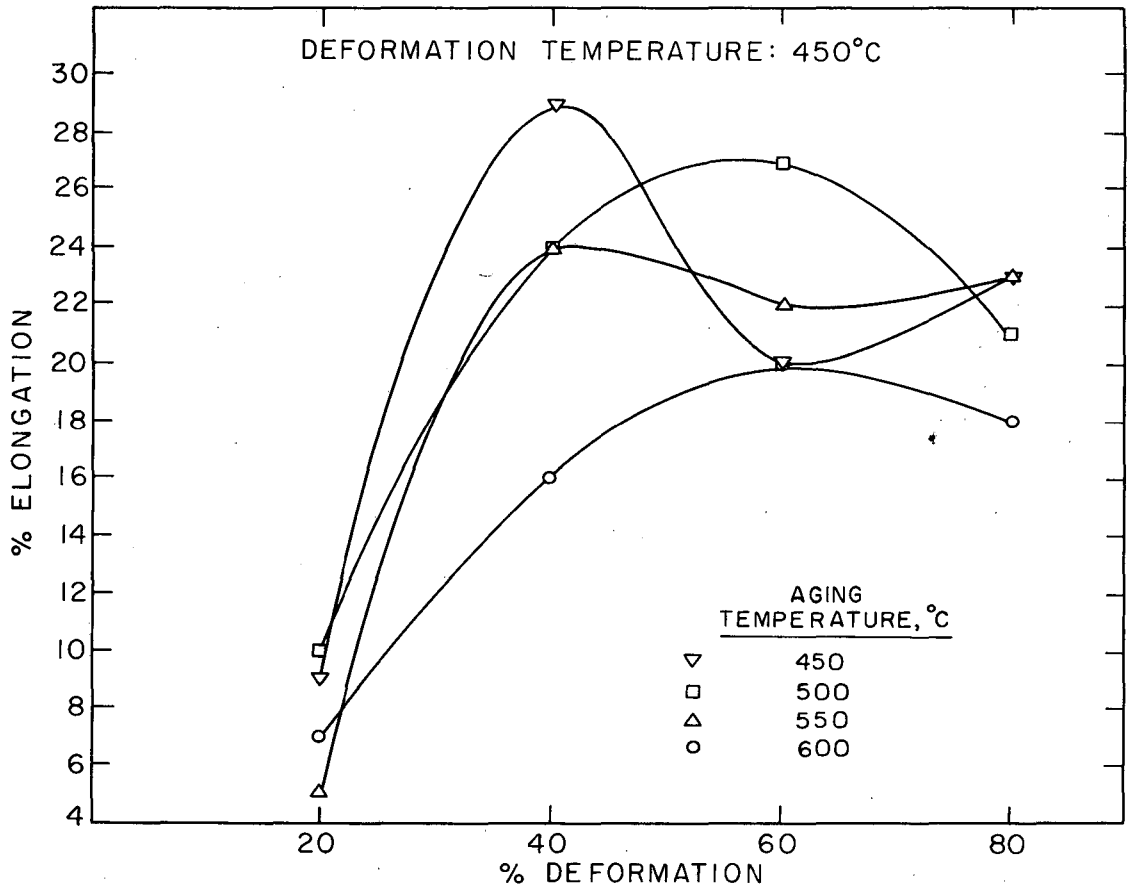

MUB-11001

Fig. 2

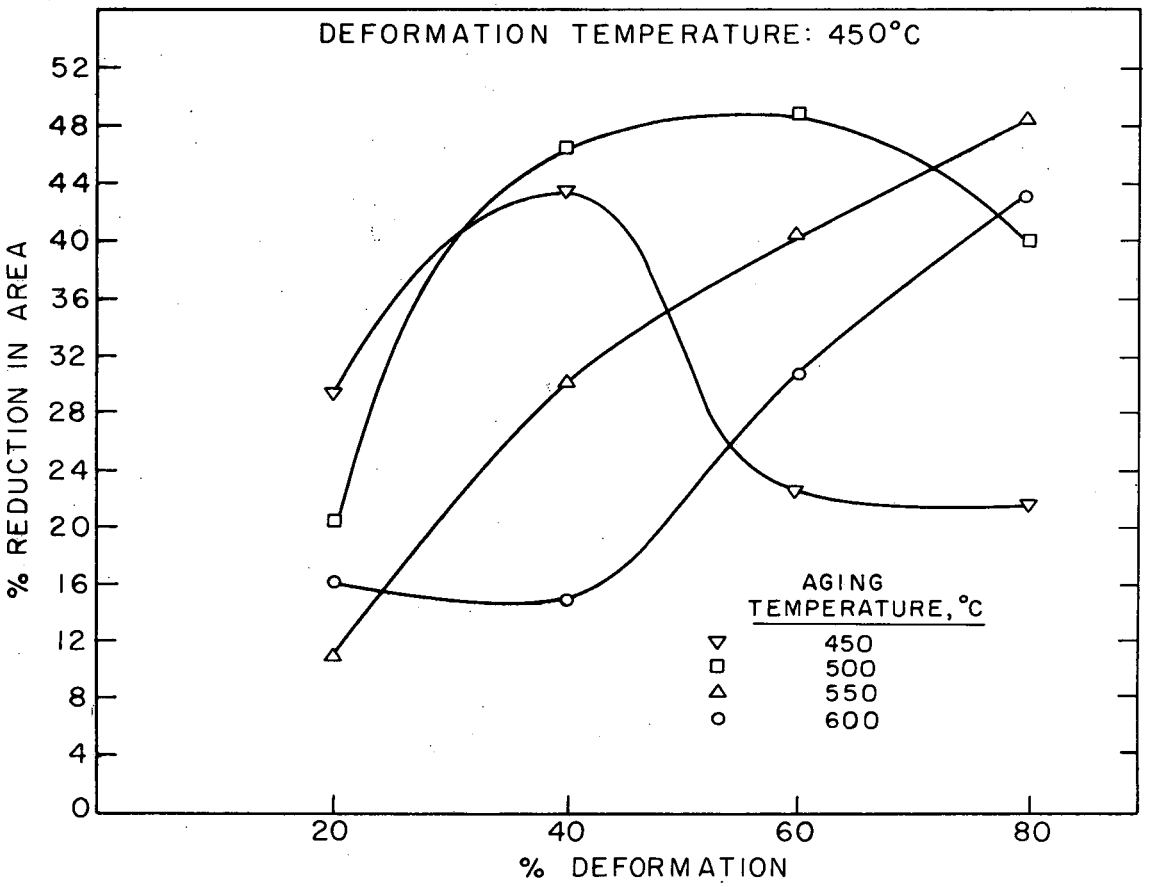

MUB-11002

Fig. 3

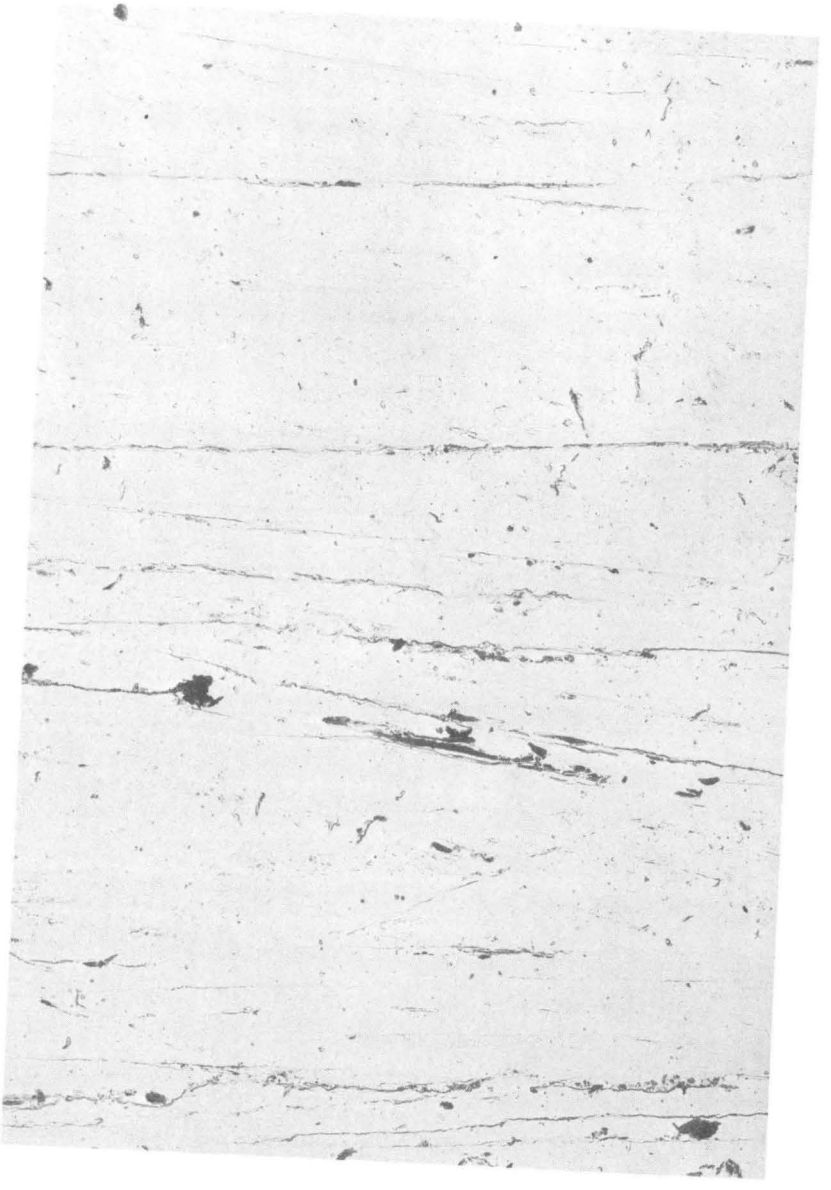

ZN 5598

Fig. 4

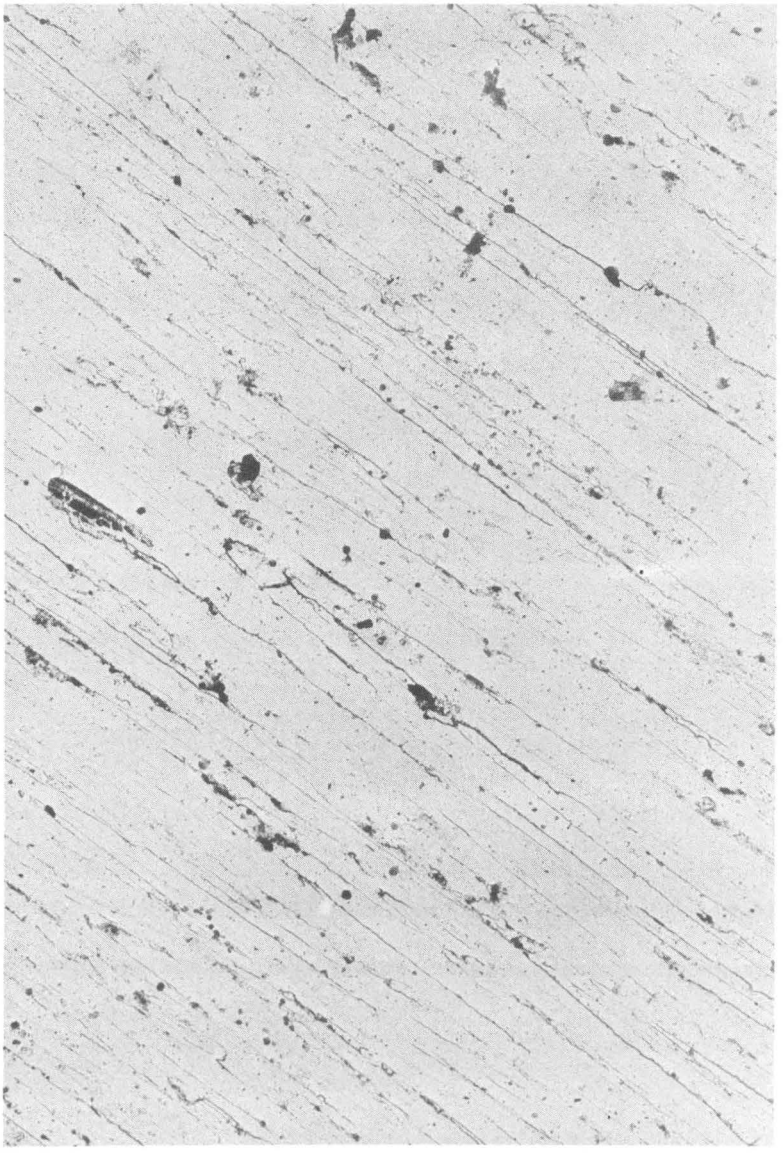

ZN 5599

Fig. 5

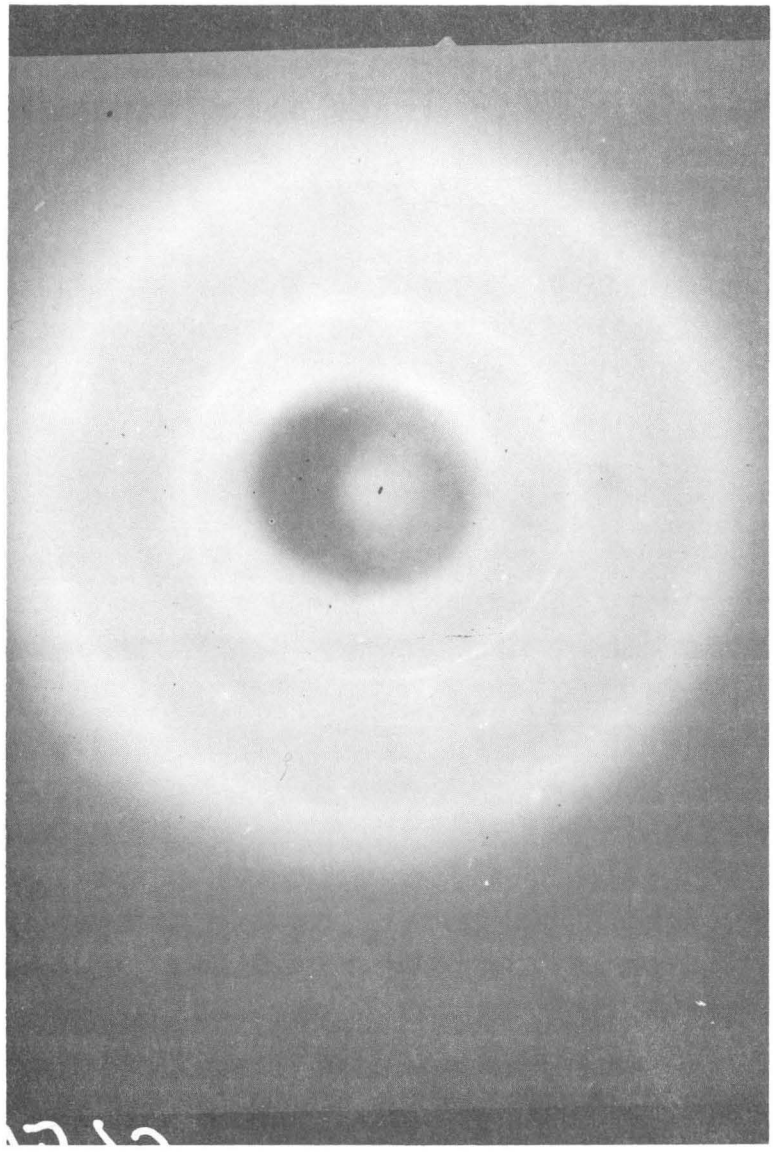

ZN 5600

Fig. 6

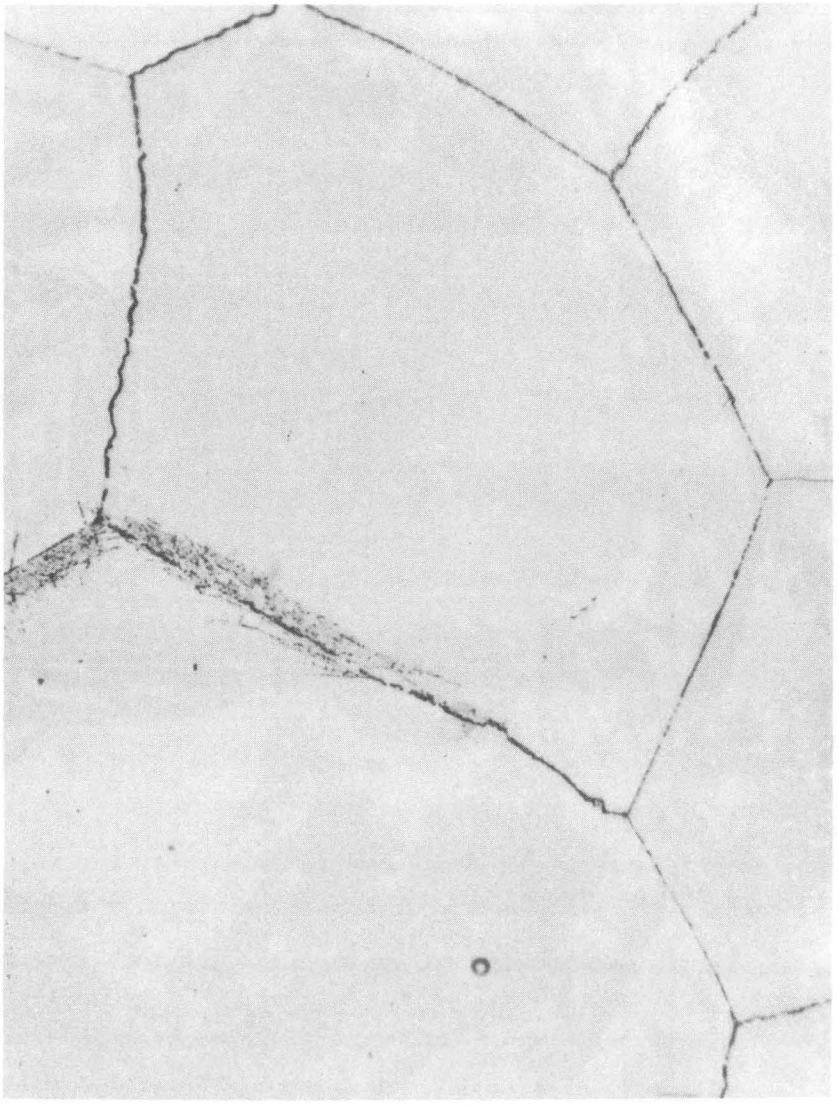

ZN 5601

Fig. 7

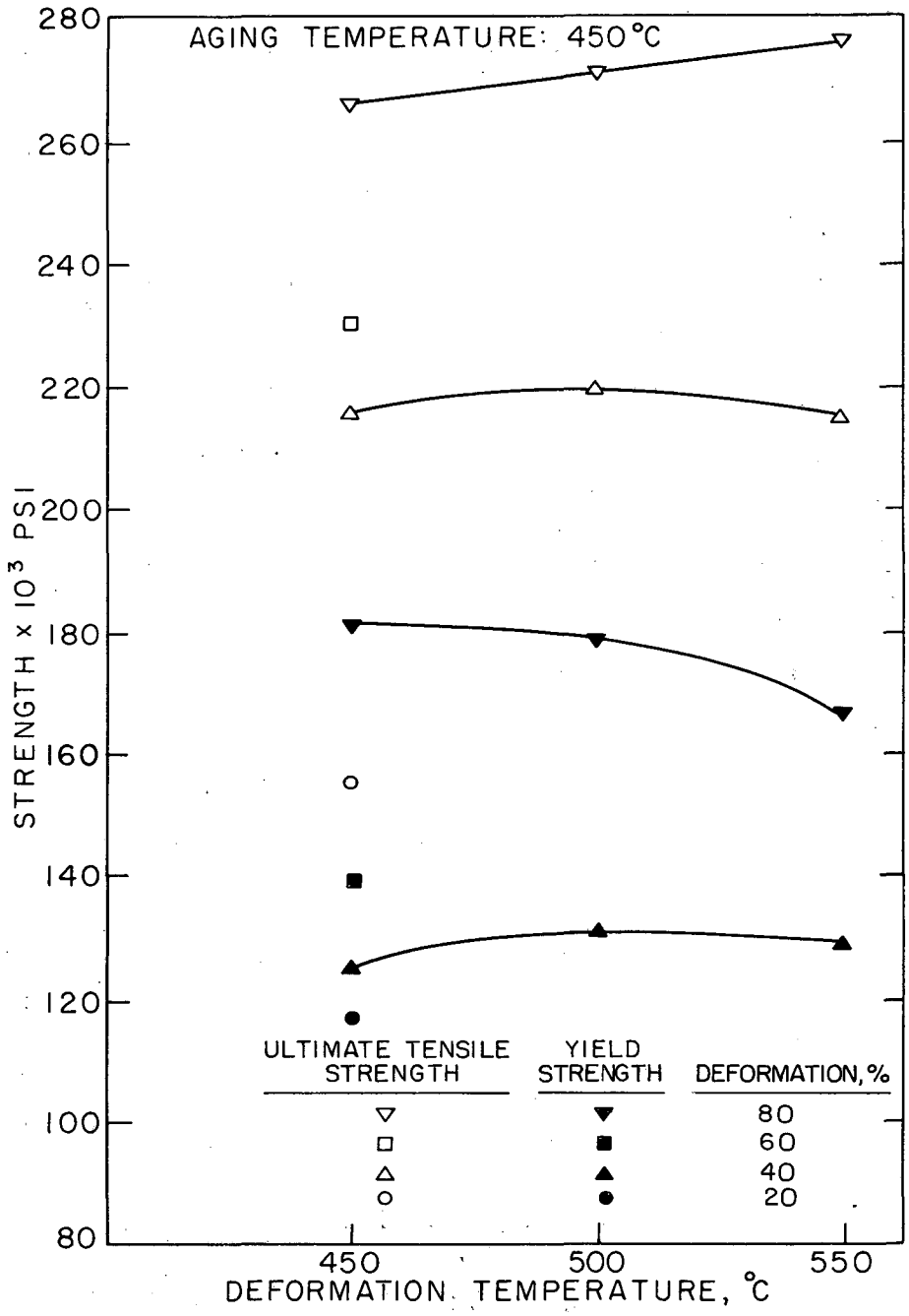

MUB-11000

Fig. 8

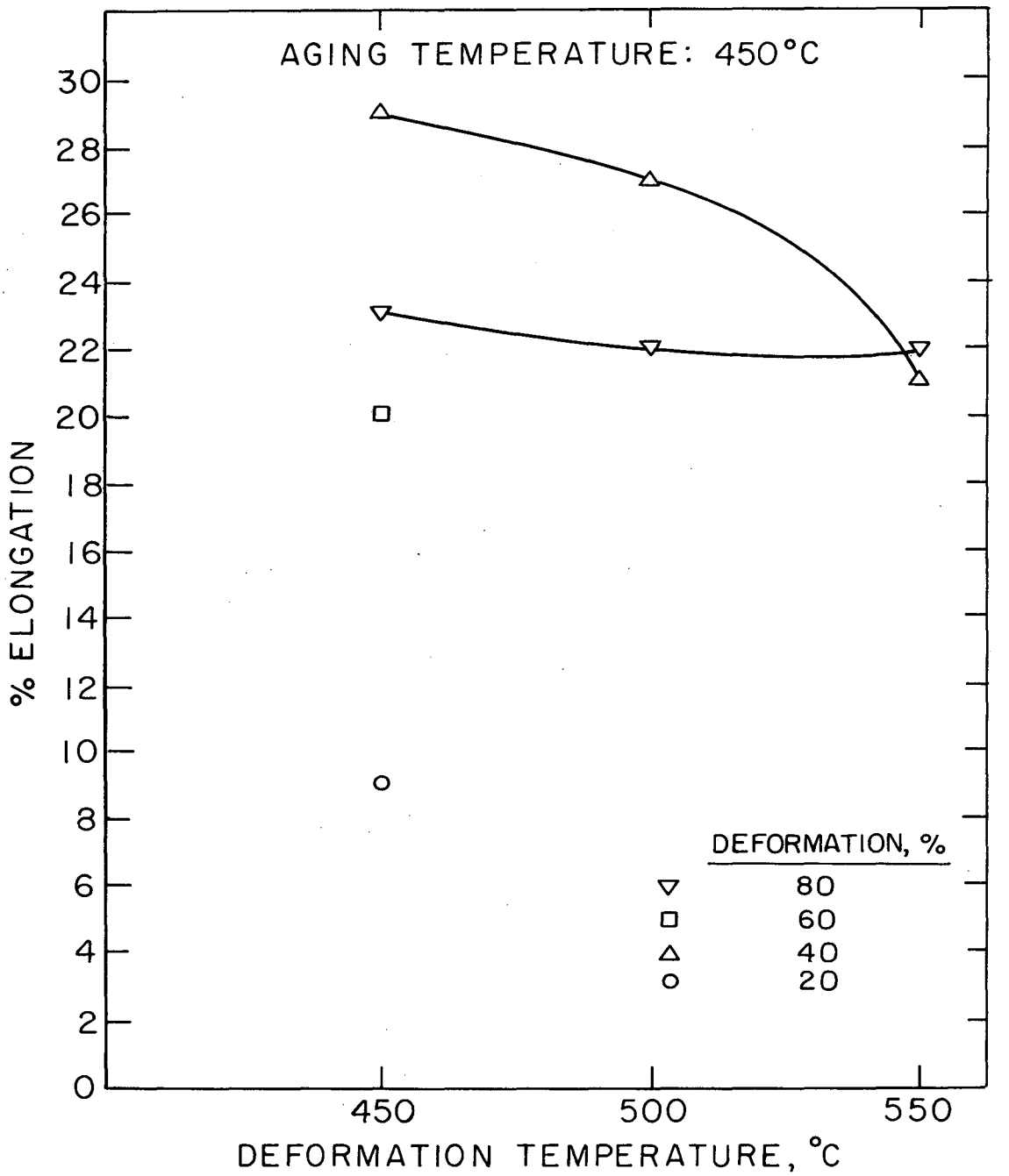

MUB-11004

Fig. 9

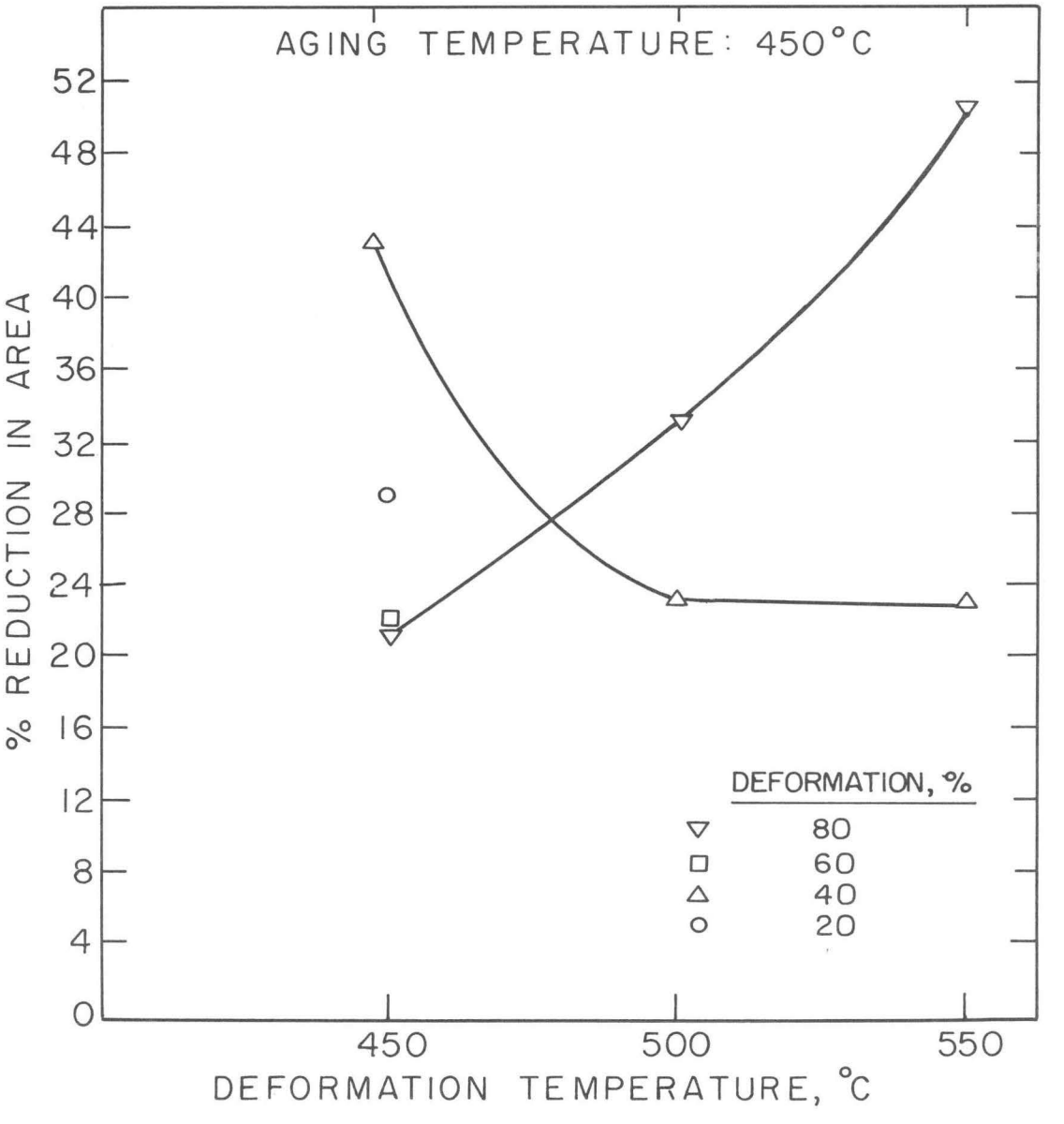

MUB-11003

Fig. 10

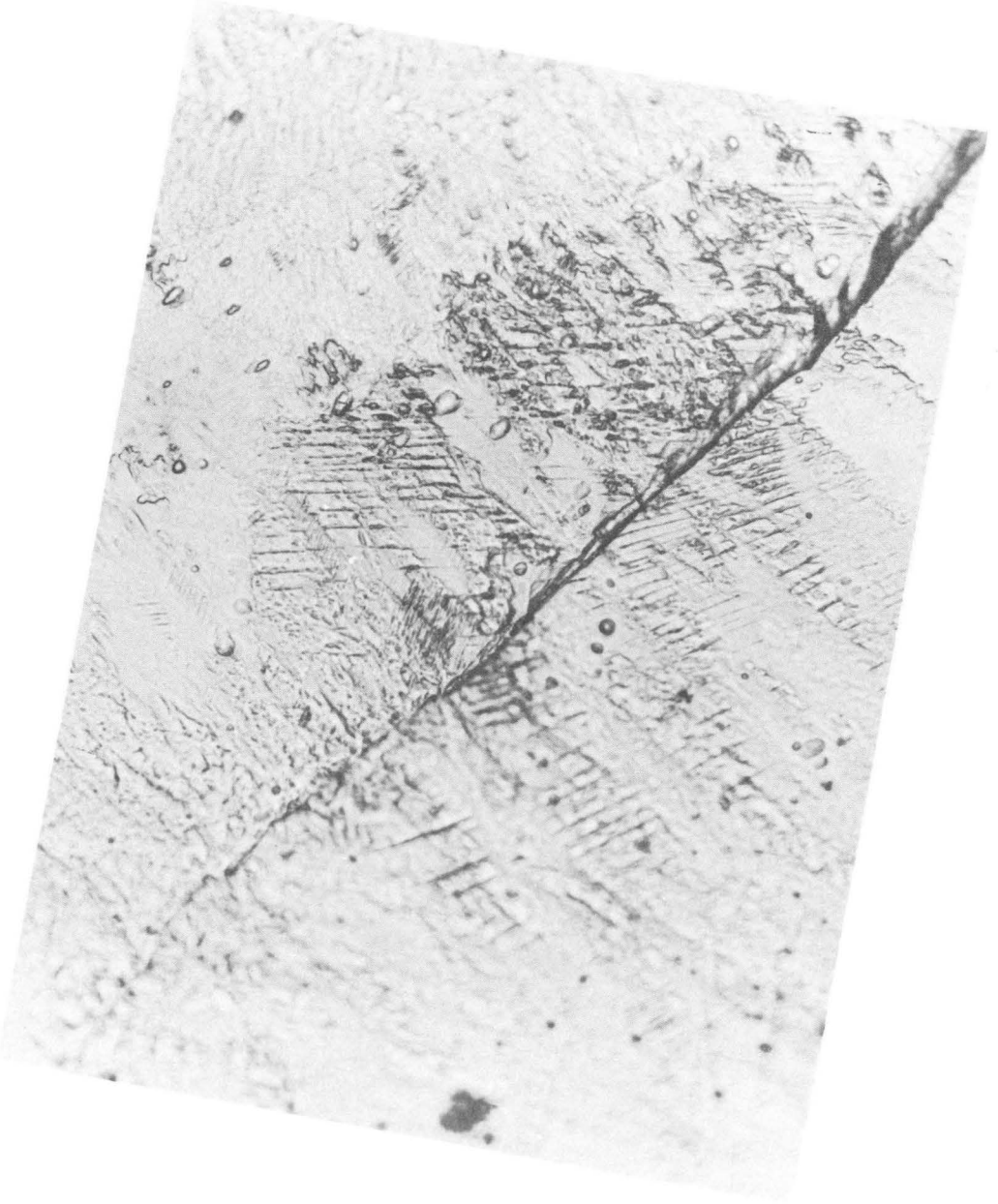

ZN 5602

Fig. 11a

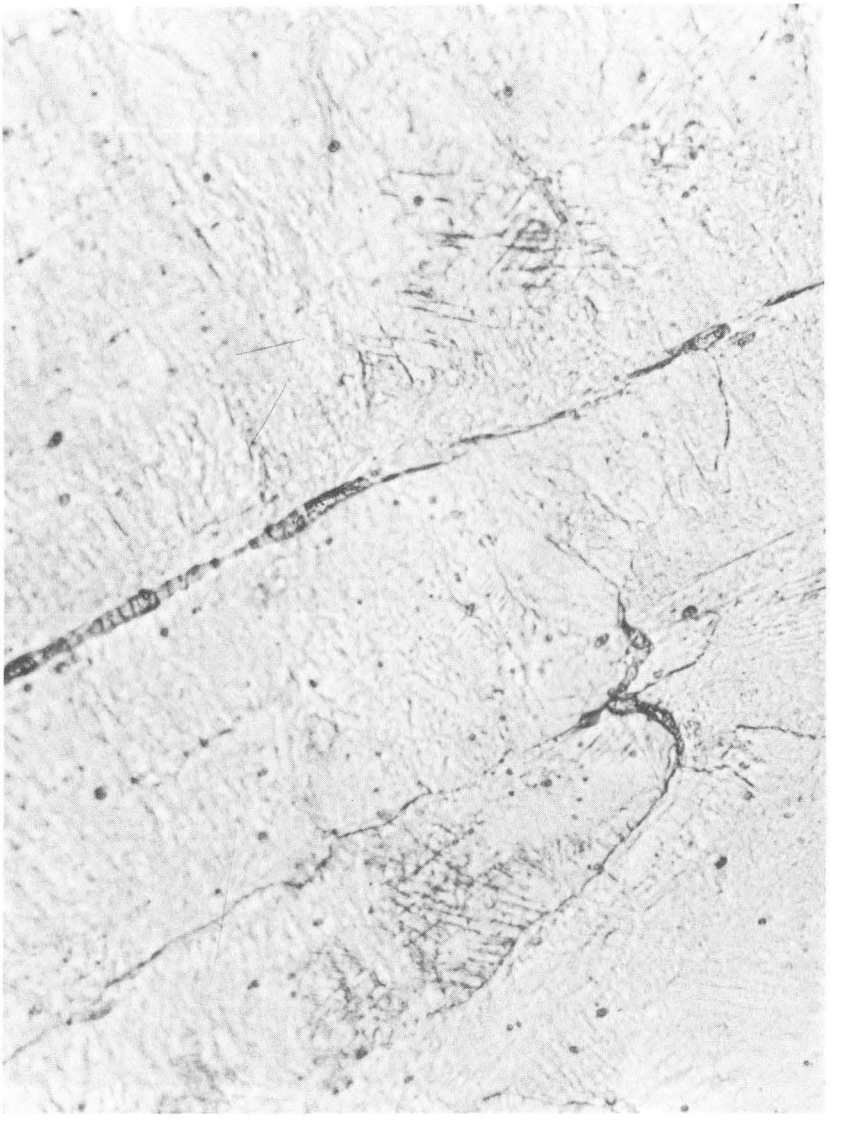

ZN 5604

Fig. 11b

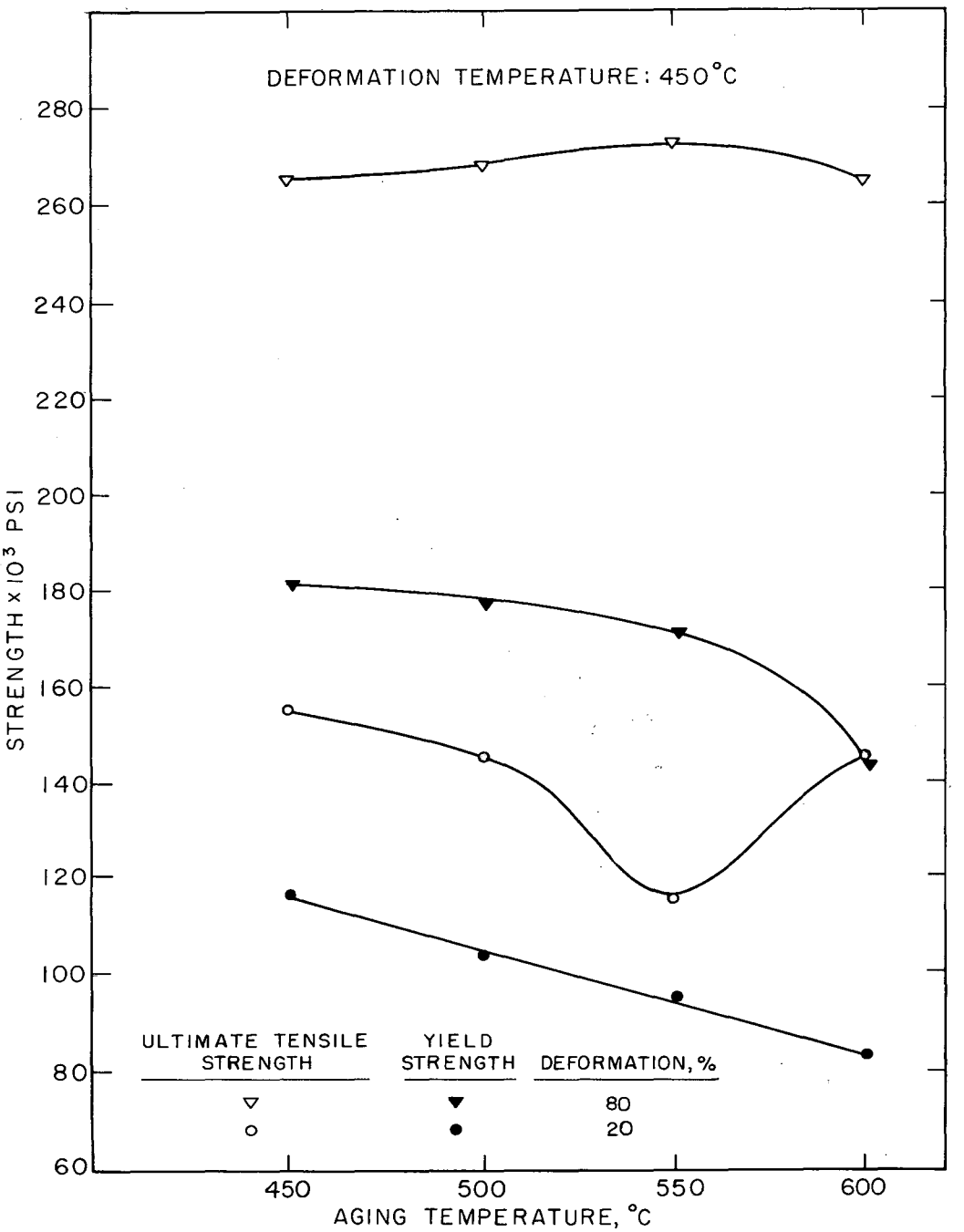

MUB-10997

Fig. 12

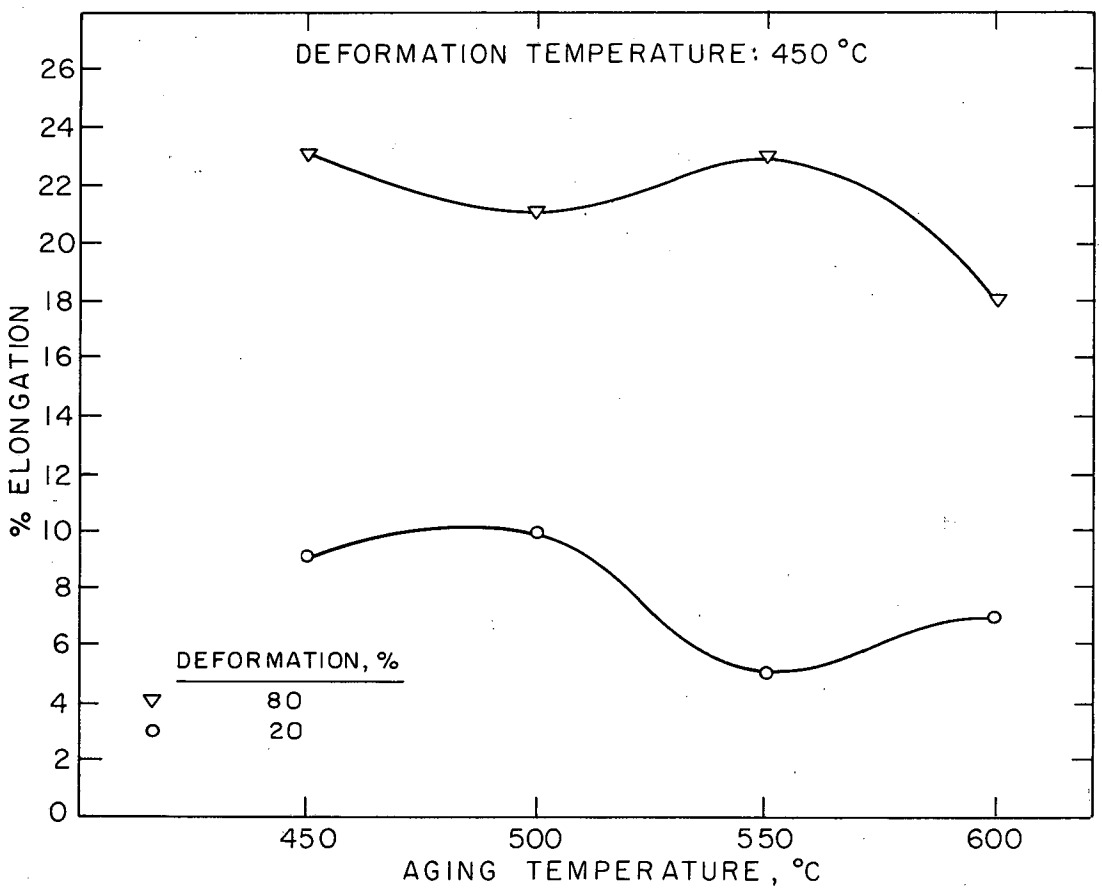

MUB-10998

Fig. 13

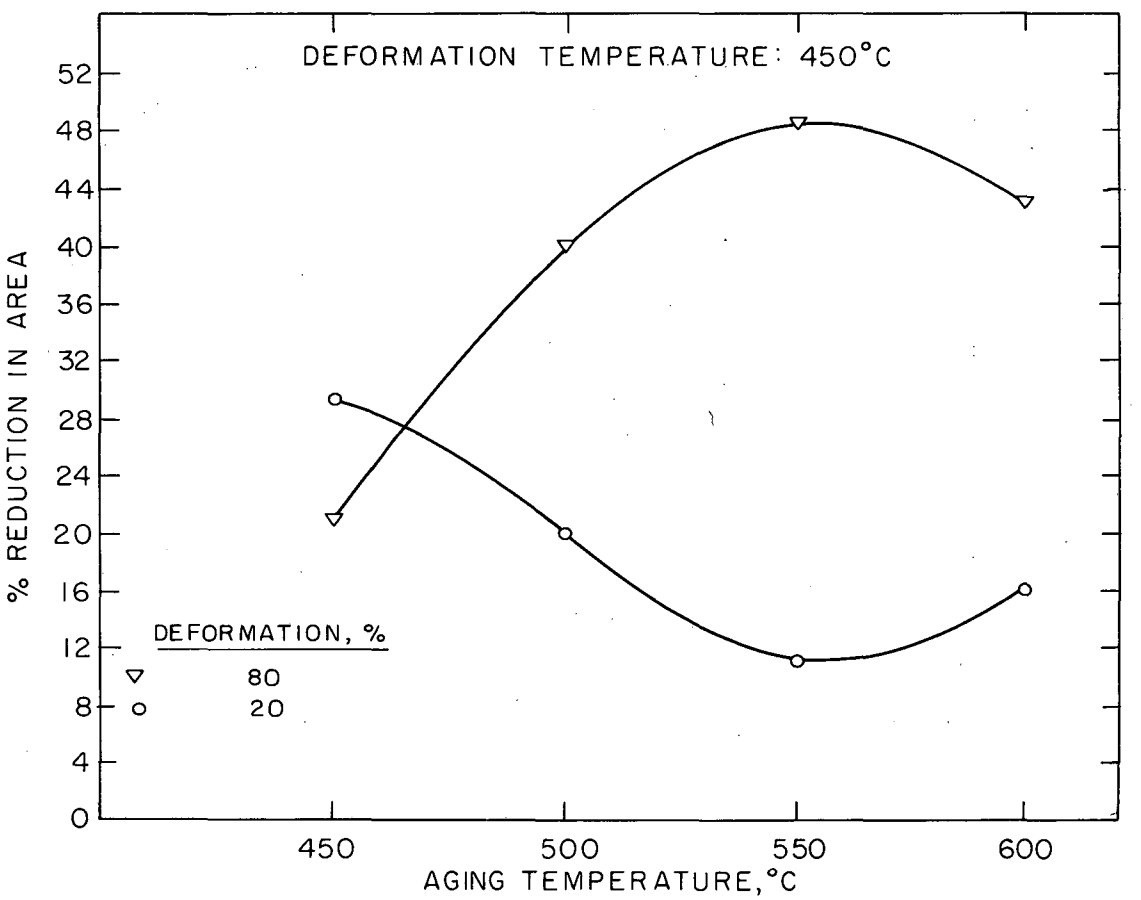

MUB-10999

Fig. 14

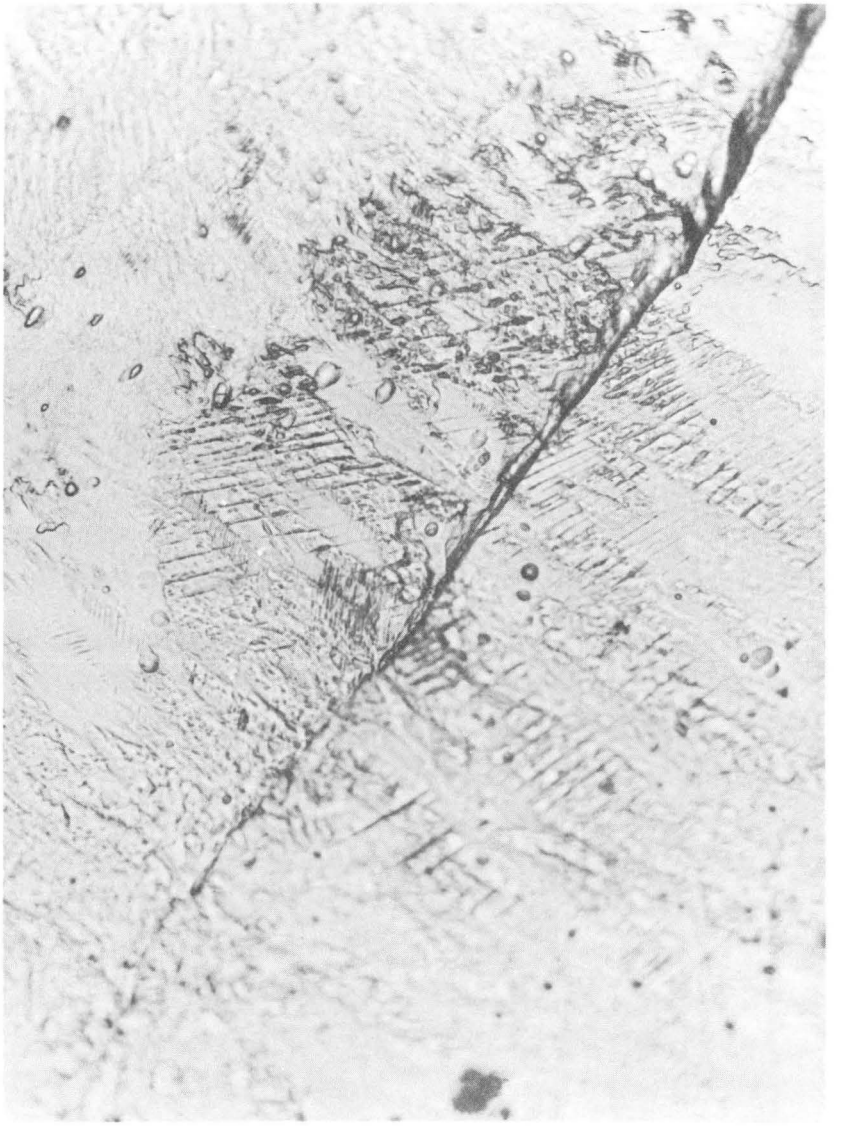

ZN 5603

Fig. 15a

ZN-5607

Fig. 15b

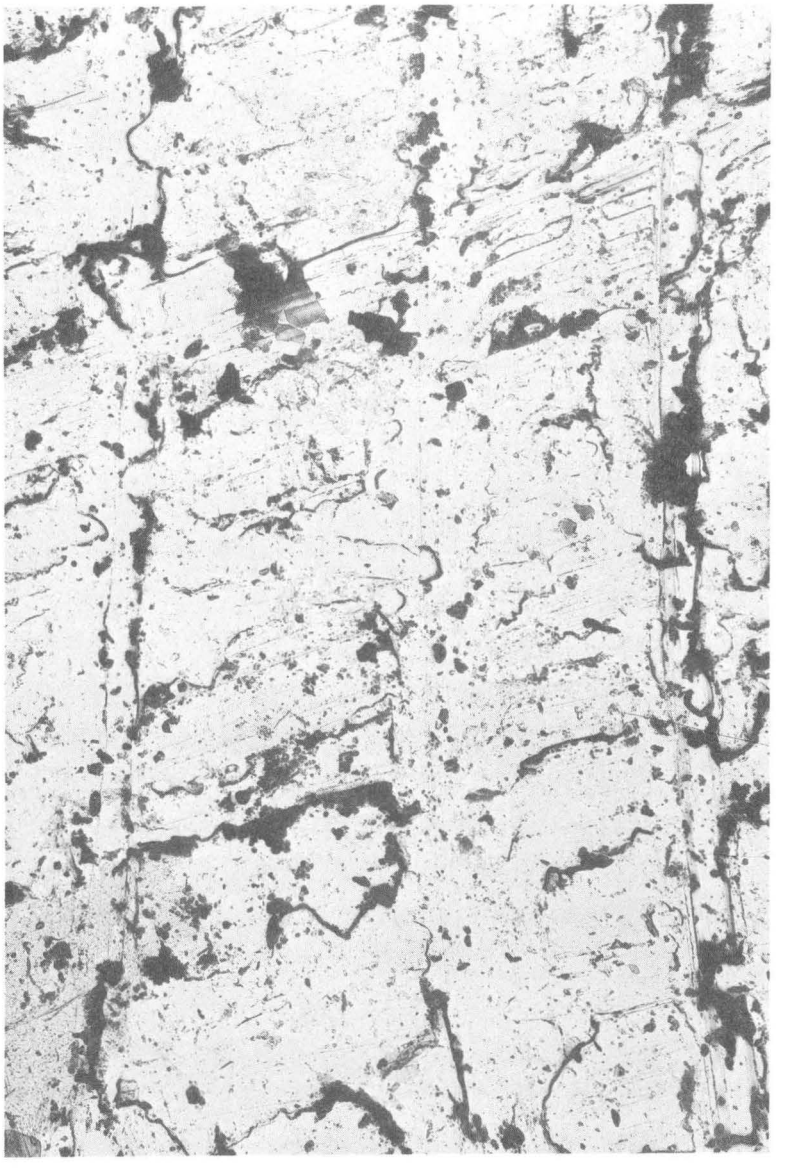

ZN-5605

Fig. 16a

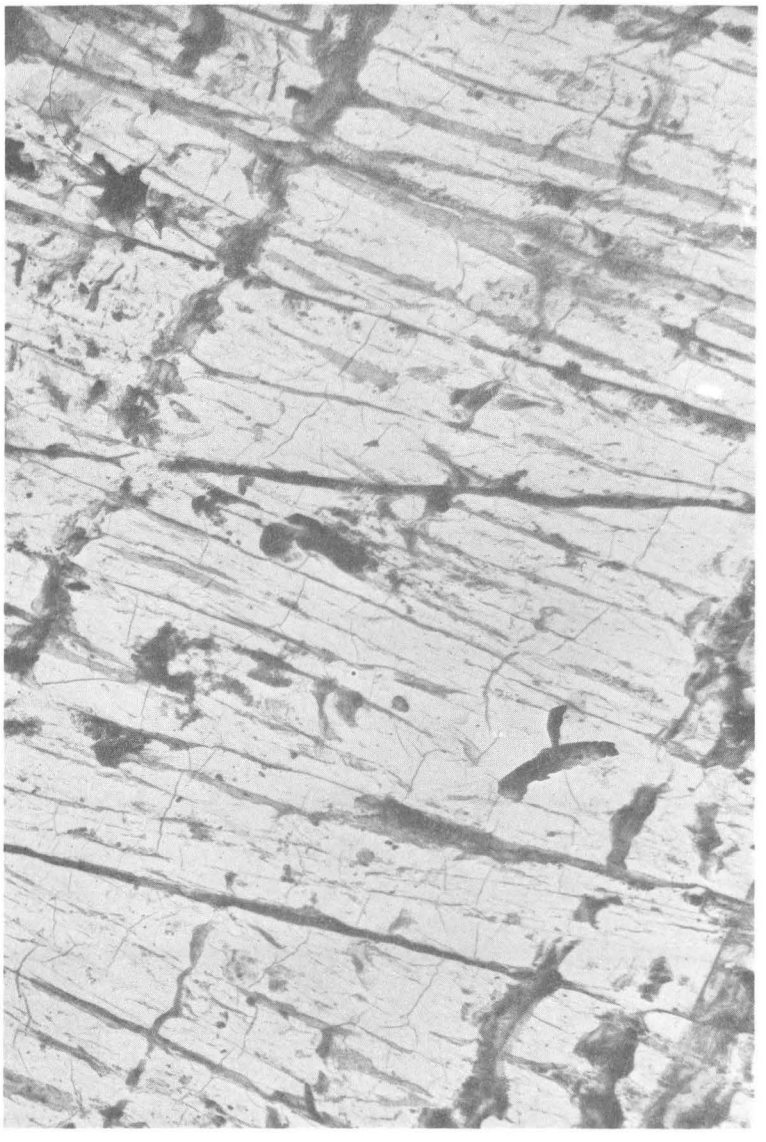

ZN 5606

Fig. 16b

This report was prepared as an account of Government sponsored work. Neither the United States, nor the Commission, nor any person acting on behalf of the Commission:

A. Makes any warranty or representation, expressed or implied, with respect to the accuracy, completeness, or usefulness of the information contained in this report, or that the use of any information, apparatus, method, or process disclosed in this report may not infringe privately owned rights; or

B. Assumes any liabilities with respect to the use of, or for damages resulting from the use of any information, apparatus, method, or process disclosed in this report.

As used in the above, "person acting on behalf of the Commission" includes any employee or contractor of the Commission, or employee of such contractor, to the extent that such employee or contractor of the Commission, or employee of such contractor prepares, disseminates, or provides access to, any information pursuant to his employment or contract with the Commission, or his employment with such contractor.